Characterization of the Coating and Tablet Core Roughness by Means of 3D Optical Coherence Tomography

Daniel Markl[1], Patrick Wahl[1], Heinz Pichler[1], Stephan Sacher[1], Johannes G. Khinast[1,2,*]

[1]Research Center Pharmaceutical Engineering GmbH, Inffeldgasse 13, Graz, Austria

[2]Institute for Process and Particle Engineering, Graz University of Technology, Inffeldgasse 13, Graz, Austria

*corresponding authors electronic address: khinast@tugraz.at

ABSTRACT

This study demonstrates the use of optical coherence tomography (OCT) to simultaneously characterize the roughness of the tablet core and coating of pharmaceutical tablets. OCT is a high resolution non-destructive and contactless imaging methodology to characterize structural properties of solid dosage forms. Besides measuring the coating thickness, it also facilitates the analysis of the tablet core and coating roughness. An automated data evaluation algorithm extracts information about coating thickness, as well as tablet core and coating roughness. Samples removed periodically from a pan coating process were investigated, on the basis of thickness and profile maps of the tablet core and coating computed from about 480,000 depth measurements (i.e., 3D data) per sample. This data enables the calculation of the root mean square deviation, the skewness and the kurtosis of the assessed profiles. Analyzing these roughness parameters revealed that, for the given coating formulation, small valleys in the tablet core are filled with coating, whereas coarse features of the tablet core are still visible on the final film-coated tablet. Moreover, the impact of the tablet core roughness on the coating thickness is analyzed by correlating the tablet core profile and the coating thickness map. The presented measurement method and processing could be in the future transferred to in-line OCT measurements, to investigate core and coating roughness during the production of film-coated tablets.

Keywords: Optical coherence tomography, solid oral dosage form, coating, roughness, 3D thickness map

1. INTRODUCTION

Although tablet coating is a well-established unit operation in the pharmaceutical industry, the achievable quality of coating is still limited by the fact that it is a highly complex process, which depends on many parameters. Slight changes of the coating equipment and process parameters may impact the physicochemical properties of the film, and consequently, affect the coating quality. The key descriptors of coating quality, particularly for functional coatings, are film coating thickness and its uniformity. Another important parameter of the dosage form is the roughness of the tablet core and of the coated tablet. It is well known that the roughness of uncoated tablets affects friability (Riippi et al., 1998) and polymer adhesion (Felton, 2013; Rowe, 1978). Surface roughness is further related to the porosity (Bawuah et al., 2014; Rowe, 1978), and thus to the disintegration and dissolution behavior of the tablets. Moreover, the roughness of a film-coated tablet influences the gloss and permeability of the film. The roughness of the tablet core, as well as of the coated tablet, thus impact the dosage form's properties and its performance. Therefore, measuring the roughness of the uncoated and coated tablet will help to better understand the impact of changes to process parameters and modifications of the formulation on the performance of the solid dosage form.

Surface roughness was previously investigated using stylus instruments (Rowe, 1979; 1978), optical microscopy (Seitavuopio et al., 2003), laser profilometer (Seitavuopio et al., 2003), scanning electron microscopy (SEM) (Riippi et al., 1998; Seitavuopio et al., 2006), atomic force microscopy (AFM)

(Seitavuopio et al., 2003) and UV imaging (Klukkert et al., 2015). However, these techniques do not allow the characterization of the roughness of the uncoated, and of the coated, tablet simultaneously at the same position. The simultaneous measurement of the roughness of both interfaces enables the analysis of the impact of the tablet core roughness on the coating uniformity, as well as on the roughness of the film coated tablet. Moreover, most techniques are time-consuming and do not facilitate the measuring of a large number of tablets, which is required to calculate significant statistical parameters.

The most promising methods to study the roughness of tablet cores and film coatings are optical imaging methods, such as confocal laser scanning microscopy (CLSM) and optical coherence tomography (OCT). Ruotsalainen et al. (Ruotsalainen et al., 2003) used CLSM to study the tablet core/coating interface and the surface of the film-coated tablet. They investigated the effects of spraying air pressure and short-term storage on aqueous hydroxypropyl methylcellulose (HPMC)-coated tablets containing an auto-fluorescent agent in the coating solution in order to achieve a good contrast of the coating layer when using CLSM. Recently, we and other research groups have demonstrated how OCT can be applied to measure the coating thickness of tablets (Lin et al., 2015; Markl et al., 2015a; 2015b; Zeitler et al., 2007) and pellets, (Li et al., 2014; Markl et al., 2015c) as well as to study the roughness of uncoated tablets (Juuti et al., 2009). OCT is a high-resolution imaging methodology to produce cross-sectional images of film coatings, in a non-destructive and contactless manner. This modality allows the direct measurement of the coating thickness, based on the knowledge of the refractive index of the coating. The very high acquisition rate of OCT (up to MHz depth scan rates (Wieser et al., 2010)) renders this method a promising tool for the in-line monitoring of coating processes. This has been reported for the coating of tablets in a pan coater (Markl et al., 2015a; Lin et al., 2017) as well as the coating of pellets in a fluid-bed coater (Markl et al., 2015c). Different data processing procedures have been developed to rapidly analyze the OCT measurements and to determine the coating thickness at several positions of individual tablets (Markl et al., 2015b, Lin et al., 2015). These data yield significant statistics about the uniformity of the coating as it facilitates the analysis of the intra- and inter-tablet coating variability besides the average coating thickness.

This study shows, for the first time, how to analyze the topography of a tablet core and its film-coating at the same location using OCT in a 3D mode. Such an analysis cannot be performed with traditional surface profilometers as they are not capable of providing information about structures below the surface. We employed OCT to investigate the correlation between the uncoated and coated tablet, as well as the coating thickness. This was performed by analyzing 3D OCT data of 11 samples (each consisting of 6 tablets) from different stages of a lab-scale pan coating process.

2. MATERIALS AND METHODS

2.1 Materials

350 g of round bi-convex tablets were coated in a laboratory-scale pan coater (ProCepT, Zelzate, Belgium), equipped with a 1-L drum and a Schlick spray nozzle, with a 0.8 mm tip. The tablet cores consisted of 50 mg acetylsalicylic acid, lactose monohydrate, microcrystalline cellulose, highly dispersed silicone dioxide (SiO2), starch, talc, and triacetin. The tablet cores (n = 20) had an average tablet diameter of 7.14 mm, thickness of 3.75 mm, curvature radius of 7.56 mm, and weight of 149.7 mg. The enteric coating was composed by 42.3% Eudragit L30 D-55, 1.2% triethyl citrate, 6.2% talc and 50.3% water. Pan speed, spray rate, inlet air flow rate and inlet air temperature were kept constant throughout the entire coating process at 40 min^{-1}, 1.40 g/min, 0.4 m^3/h, and 42°C, respectively. The process ran for 88 minutes, until a total mass of 120 g of coating material was sprayed onto the tablets, yielding a total coating thickness of 51.2 ± 2.8 µm (the standard deviation corresponds to the inter-tablet coating variability of 6 samples). The coating thickness as a function of process time is provided in Figure S.1 in the supplementary information. Tablet samples (each sample consists of 6 tablets) were drawn every 8 min, yielding 11 samples in total. The samples are from the coating process (B01) presented in Markl et al.(Markl et al., 2015a), whereas all tablets were measured again with the 3D OCT setup.

2.2 Optical coherence tomography

In OCT an optical beam emitted by a broadband light source (i.e., high spatial but low temporal coherence) is focused onto the surface of the sample. The main part of the light is directly reflected by the surface of the sample. A substantial fraction of the light penetrates into the coating structure and is then reflected back by subsequent interfaces, separating two media with different indexes of refraction, i.e., the coating and the core material. Therefore, coating/tablet core interface is visible if the coating layer is (i) thicker than the resolution limit of the used system (> 10 µm), (ii) the coating does not exhibit high scattering losses due to particles in a size range of the operating wavelength, and (iii) there is a change in refractive index between adjacent media (i.e., air/coating and coating/tablet core). Measuring the optical path length difference between the reflections of the coating surface and the coating/material core interface allows the determination of the coating thickness, based on the knowledge of the refractive index of the coating material.

The base OCT system presented previously in Markl et al., 2015a allows the use of two different probes, namely a 1D and 3D imaging probe. The latter was employed in this study in order to acquire 3D data of a sample of interest, in an off-line configuration. The light source operates at a central wavelength of 832 nm and has a spectral bandwidth of 75 nm, which provides a theoretical axial resolution of 4.1 µm. The 3D imaging probe allows the reconstruction of depth-resolved cross-sections, or volumes, by scanning the probing beam laterally across the sample, with the aid of galvanometer mirrors GM1 and GM2 (Cambridge Technologies), and sub-sequent acquisition of depth scans at successive lateral positions (see Figure 1). The light emerging from the fiber is split at a non-polarizing bulk beam splitter BS (splitting ratio 50/50, Thorlabs) into a reference and a probe beam. The probe beam is focused by an achromatic lens L1 (Thorlabs, focal length, f = 36 mm). This setup provides a theoretical lateral resolution of 10 µm and a depth of focus of 171 µm. The spectrometer consists of a fiber collimator FC (OZ Optics, diameter = 20 mm), a transmissive diffraction grating DG (Wasatch Photonics Inc., Logan, Utah, USA, 1200 lines/mm), an achromatic lens L3 (Thorlabs, focal length = 100 mm) and a line scan camera with a 2048 pixel CCD array (Atmel Aviiva, 14 x 28 µm² pixel size, 12 bit resolution). The output voltage of each CCD pixel is proportional to the number of photons hitting an individual pixel, accumulated during the CCD exposure time of 30 µs.

Single depth scans and cross-sections are labelled as A- and B-scans, respectively. Cross-sectional images are synthesized from successive A-scans. Moreover, three-dimensional volumetric data can be created by acquiring sequential B-scans. Throughout this study we analyzed only 3D OCT data consisting of 512 B-scans, which covers a volume of 3.12 x 3.12 x 1.6 mm³; each 2D image has a dimension of 1024 x 1024 (3.12 x 1.6 mm²). The total acquisition time per volume lasts for about 1 minute.

An automated data evaluation algorithm extracts information about coating thickness, as well as tablet core and coating roughness. This analysis can be carried out either on the basis of cross-sectional images or by using 3D data of the samples. The focus in this study is the analysis of 3D images of the samples removed periodically from a pan coating process. A thickness map and profile maps of the tablet core and coating are computed from about 480,000 depth measurements per sample. This data enables, among others, the calculation of statistical roughness parameters of the assessed profiles.

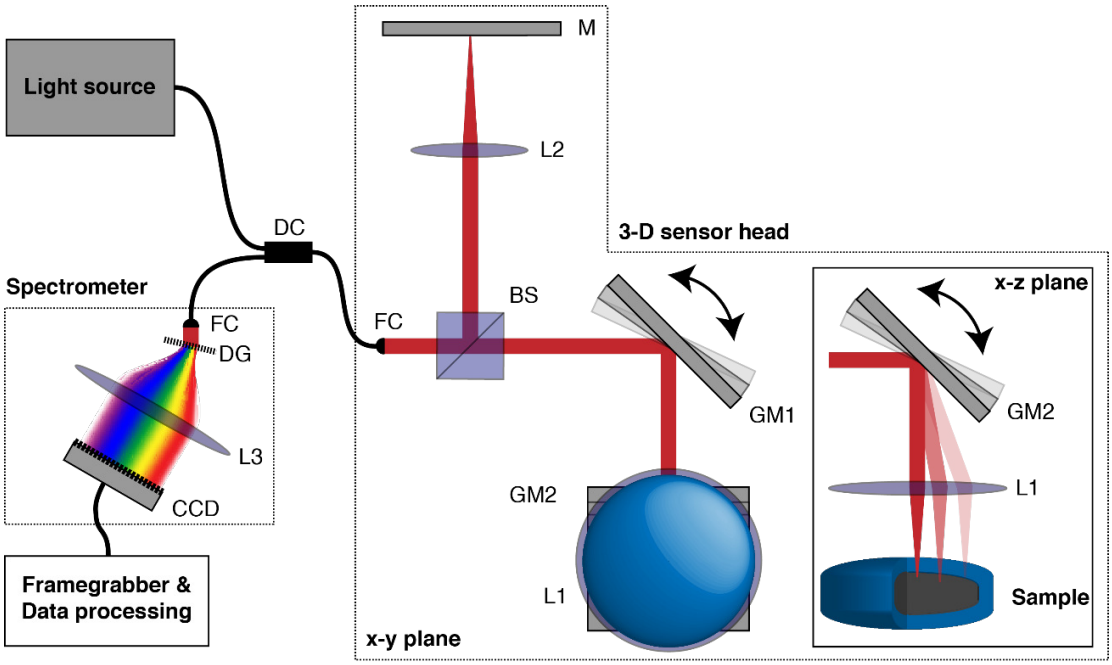

Figure 1: Schematic of OCT system for a 3D and 1D sensor head. DC – directional coupler, FF – fiber focuser, BS – beam splitter, M – mirror, FC – fiber coupler, DG – diffraction grating, Lx – lens, CCD – charged coupled device, GMx – galvanometer mirror. This schematic was modified from Markl et al., 2015a.

137

138 ### 2.3 Roughness Analysis

139 A surface profile is in general defined as the result of an intersection between the surface and a defined
140 plane (Figure 2). In the case of OCT, this plane is a B-scan, which was acquired perpendicular to the
141 tablet face. The data evaluation procedure developed for the coating thickness analysis of 2D OCT
142 images was applied on the 3D volume data. This algorithm was presented in Markl et al. and consists
143 of four stages: (1) converting the raw spectra to image data by applying a non-uniform Fourier
144 transform (Markl et al., 2015b), (2) detecting the air/coating and coating/core interfaces, (3) correcting
145 the coating/core interface from distortions induced by the refraction of the beam on the air/coating
146 interface, and (4) determining the coating thickness. The application of the algorithm on each B-scan
147 of the 3D data allows the generation of a coating thickness map. Moreover, these data facilitate the
148 determination of coating and core profiles from the detected coating interfaces. The coating and core
149 profiles represent the deviations of the air/coating and coating/core interfaces from their respective
150 mean lines. The mean lines of both interfaces are assumed to follow a circle due to the bi-convex shape
151 of the tablets. Consequently, analyzing the roughness of bi-convex tablets requires the determination
152 of the deviations of the actual surface from a circle with a specified radius and center. A circle was
153 therefore fitted in each detected interface and each point on the interface was represented by a polar
154 coordinate, as schematically shown in Figure 2 for the air/coating interface. The radius of the fitted
155 circle was then subtracted from the radial coordinate, yielding the coating and core profiles.

156 The calculated deviation in height of the interfaces from the fitted circle is the surface roughness of
157 the interface. Roughness is typically expressed by statistical parameters, as defined in international
158 standards (e.g., DIN EN ISO 4287). One of the most common descriptors is the root mean squared
159 deviation, which can be expressed as

$$Rq = \sqrt{\frac{1}{N}\sum_{i=1}^{N} y_i^2} \tag{2.1}$$

with y_i as the surface height at measurement position i (see Figure 2) and N as the total number of measurements. Other statistical parameters are skewness (Rsk) and kurtosis (Rku), which are defined as

$$Rsk = \frac{1}{Rq^3 N}\sum_{i=1}^{N} y_i^3 , \tag{2.2}$$

$$Rku = \frac{1}{Rq^4 N}\sum_{i=1}^{N} y_i^4 . \tag{2.3}$$

Skewness measures the profile symmetry about the mean line and kurtosis is a descriptor of the sharpness of the profile. A negative Rsk represents a surface which mainly consists of valleys, whereas a positive value indicates that the surface is predominantly peaks. The kurtosis is a measure for the sharpness of the profile, where a spiky surface will have a high kurtosis value.

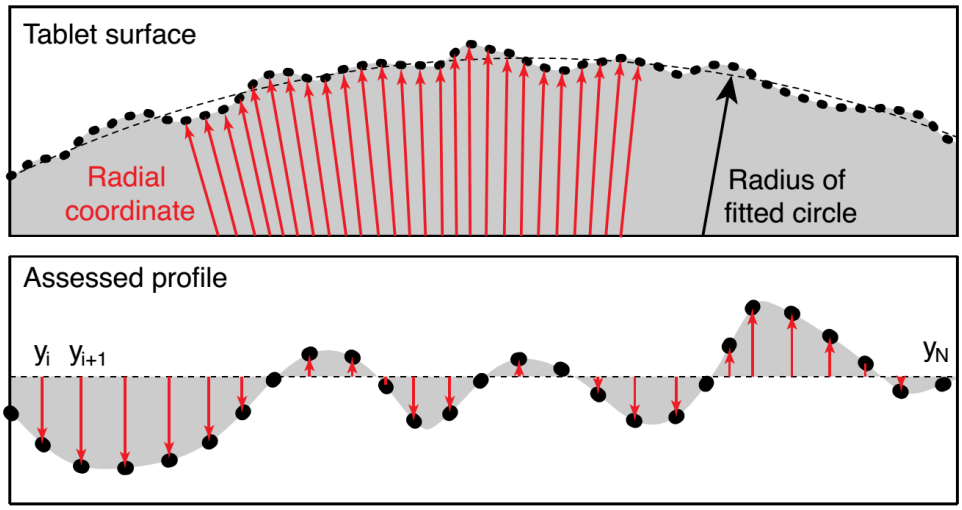

Figure 2: Schematic of the coating profile generation from the detected air/coating interface. y_i is the height of the surface profile at position i for a total of N measurements. Each point on the tablet surface is represented by a radial coordinate. The profile is assessed by subtracting the radius of the fitted circle from the radial coordinate.

2.4 Validation of OCT profile measurements

The OCT roughness analysis was validated by roughness maps generated by a contact profilometer (Veeco DEKTAK 150), using a 0.9 µm radius tip which can provide a vertical resolution of up to 1 Å. The contact profilometry measurements were performed on the tablet surface covering a range of 3 x 3 mm² (250 x 3000 px). The acquisition time per profile map was about 1 hour.

3. Results and discussion

3.1 Comparison of OCT and contact profilometry

Figure 3 shows 2D roughness maps of one film-coated tablet, by means of contact profilometry and OCT. Both measurements are in very good agreement, which is also indicated by the statistical roughness parameters listed in Table 1 and by the frequency distribution in Figure 4. Slight deviations between the profilometer and OCT measurements are due to the different instrument settings (i.e., scanning range, vertical and horizontal resolution) and due to a slight rotation of the tablet between the two measurements. Moreover, the OCT data suffers from minor distortions which are mainly due to the so-called fan distortion, which is related to the rastering of the surfaces using optical scanners (e.g. galvanometer mirrors). This effect curves the OCT image deeper and it is stronger the farther away from the center. Fan distortion can be corrected by a three-dimensional distortion correction algorithm as proposed by Ortiz et al., 2010.

Table 1: Statistical roughness parameters from contact profilometry and OCT of the same tablet (sample from process time 88 mins). The data is shown in Figure 3.

		Contact profilometry	OCT
Rq	µm	3.98	4.09
Rsk	-	-0.23	-0.23
Rku	-	3.95	4.32

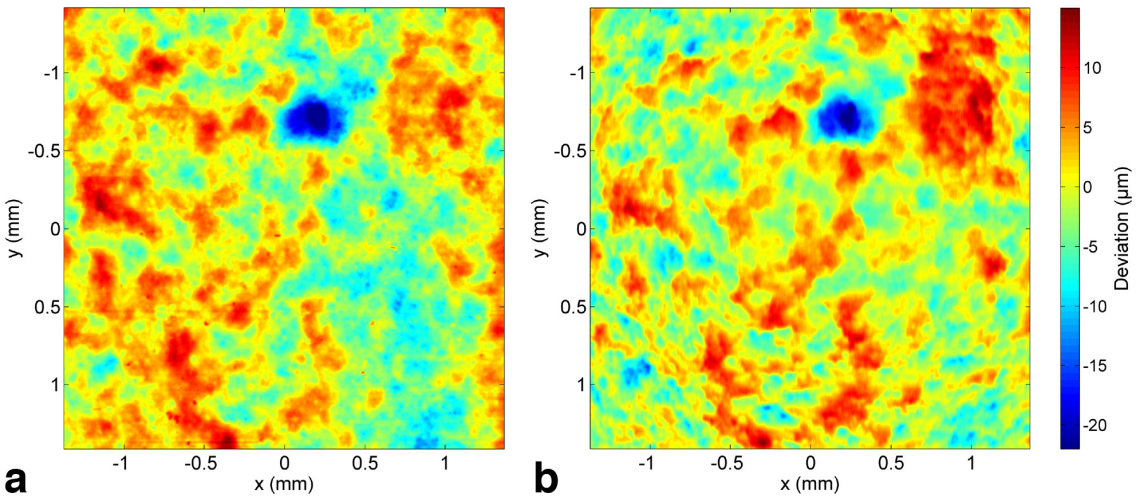

Figure 3: 2D roughness maps of a final film-coated tablet at the same position using (a) contact profilometry and (b) 3D OCT. The color bar is valid for both figures. The statistical roughness parameters of both measurements are given in Table 1.

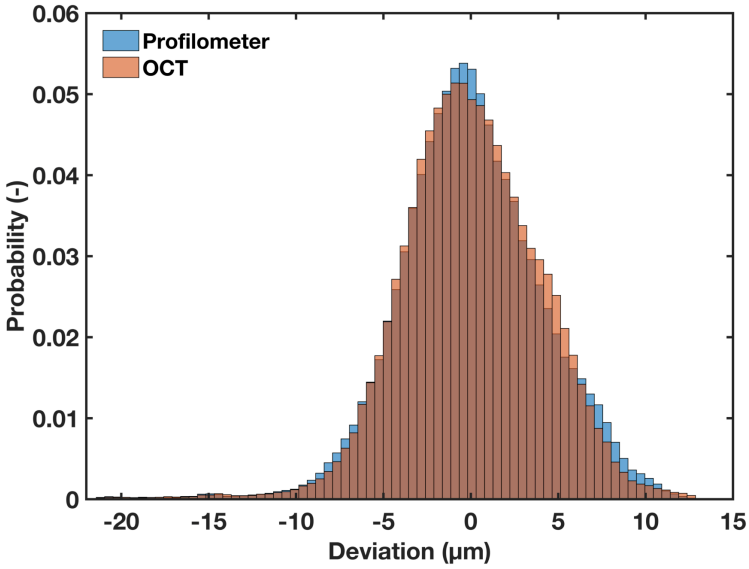

Figure 4: Frequency distributions of the roughness measurements using OCT and the profilometer. The frequency distributions were calculated from the 2D roughness maps as depicted in Figure 3.

194

195 **3.2 Correlation between coating profile, tablet core profile and coating thickness**

196 In the following we focus on the results from the OCT measurements, allowing the measurement of a
197 much larger number of tablets due to the high acquisition rate, as well as due to the advantage of
198 measuring the coating and the tablet core profile simultaneously (Figure 5). Further results are shown
199 in Figure S.2 in the supplementary information. Comparing the core and the coating profiles reveals
200 that small valleys of the tablet core profile are filled with coating. However, larger valleys and peaks in
201 the core are still present in the coating.

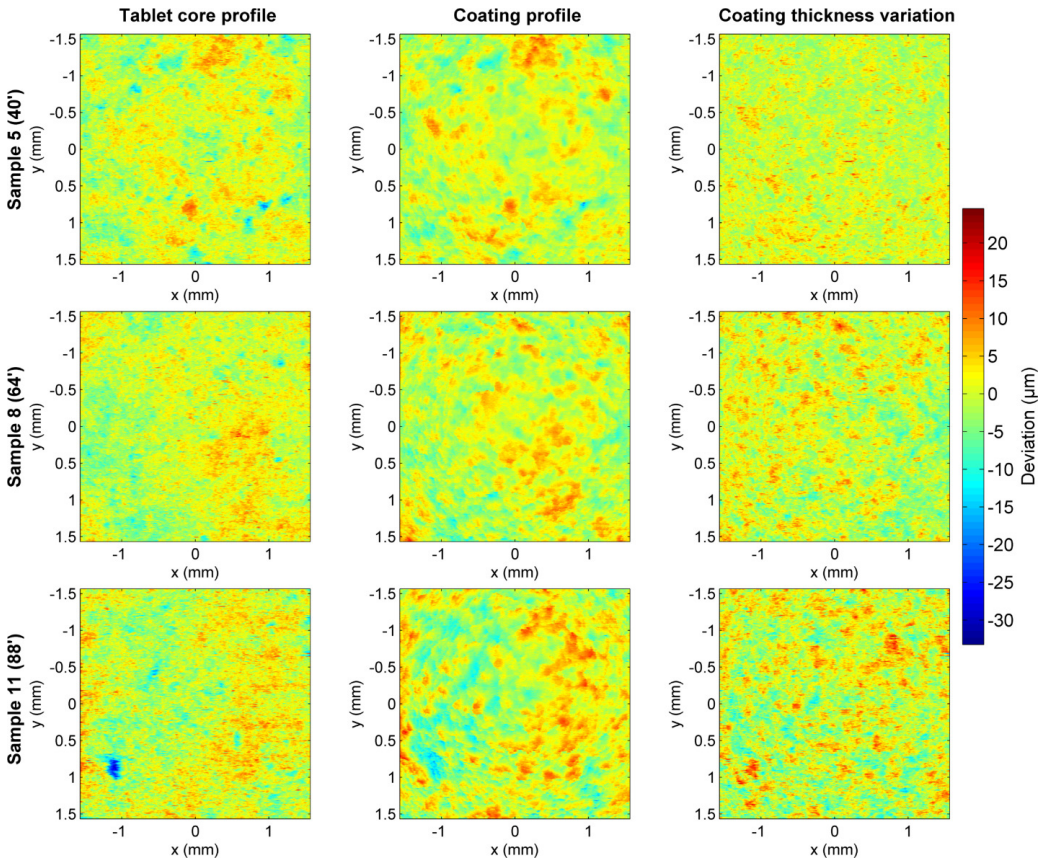

Figure 5: Tablet core and coating profiles, as well as coating thickness variations, of three tablets from different stages of the coating process. Each row corresponds to the same OCT measurement. The dimensions of each map are 3.12 x 3.12 mm^2 (512 x 1024 pixels).

A more detailed investigation of the relation between the core profile, coating profile and the coating thickness can be performed by calculating correlation coefficients (Figure 6). As expected, a weak linear correlation (coefficient close to 0) at the early stages of the coating process can be observed for the core profile/coating thickness. This is also true for the coating profile and coating thickness. On the contrary, the coating profile and the core profile are highly correlated, i.e. both profiles are almost identical, as the coating is still very thin and thus below the resolution limit of OCT at this stage of the process. The most significant changes of the coefficients occur in the first half of the coating process (< 48 min), where the average coating thickness is < 28 µm. The correlation coefficient between the coating and core profile approaches 0.5, which evidences that the final coating profile still represents features from the original core profile. The negative correlation coefficient of the core profile and coating thickness variation reflects a negative linear dependence between these two variables, which indicates that a valley or a peak in the core profile causes a larger or smaller coating thickness, respectively.

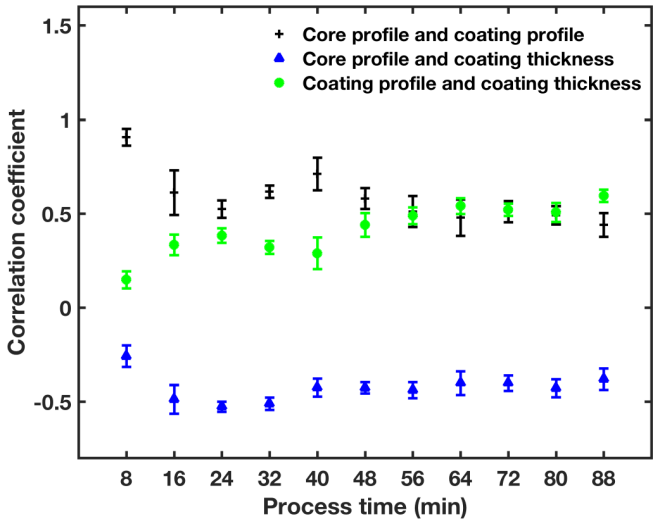

Figure 6: Correlation coefficients between core profile, coating profile and thickness variation maps depending on the process time. Each data point is the average correlation coefficient of 6 tablets and the error bar corresponds to its standard deviation. The size of each map used for the calculation of the correlation coefficients were 3.12 x 3.12 mm^2 (512 x 1024 pixels).

3.3 Statistical roughness parameters

The correlation of the different profiles can be further analyzed on the basis of the statistical roughness parameters (Rq, Rsk and Rku). The root mean square deviation for the coating and the core profile is illustrated in Figure 7a. Rq deviates at the beginning of the process ($<$ 24 min) from the values at the end of the process, even though the roughness of the tablet cores should be similar throughout all measurements. We want to remind the reader at this point that tablets were drawn from the process at each stage for the analysis and they were not returned to the process. Although the tablet cores are from the same batch, the roughness of the tablet cores clearly varies as indicated by the standard deviation of the tablet core Rq as well as by the difference in average Rq between each process stage. The coating roughness is constant towards the end of the process in contrast to the tablet core roughness, which indicates that the coating process compensates, to a certain extent, the roughness variations of the tablet cores. Moreover, the timely deviation of the tablet core Rq is primarily due to the thin coating layer (15 µm at 24 min) at the beginning of the process, which cannot be accurately resolved by the OCT system in use, causing a misdetection of the tablet core interface. The large standard deviation at process time 40 min is due to a defect, which is discussed below on the basis of the kurtosis.

However, the roughness of the tablet at process times < 48 min is higher than that of the coating surface, as the coating droplets preferentially fill in irregularities in the tablet core which causes a smoother surface (Figure 7). On the contrary, the coating is slightly rougher than the core towards the end of the process. The roughness of the coating surface strongly depends on the coating application conditions, as was shown by Twitchell et al., 1995. The authors stated, on the basis of light section microscope measurements, that increasing the spray gun-to-bed distance, changing the spray shape from a narrow cone to a wide flat spray or decreasing the atomizing air pressure produce rougher surfaces.

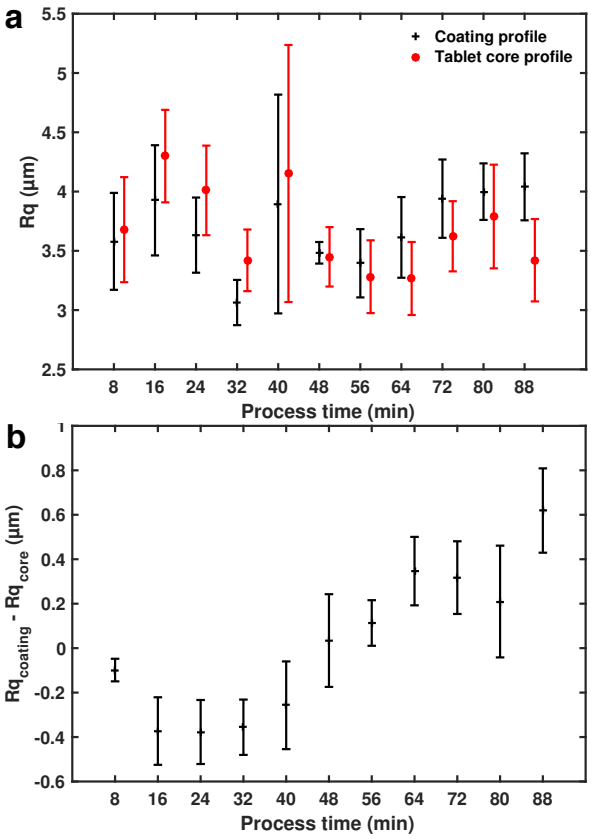

Figure 7: Analysis of the root mean square deviation as a function of process time. (a) Average $Rq \pm$ standard deviation (errorbar) for each profile. The process time of the tablet core profile was shifted by 2 min in order to enhance the visibility of all data points. (b) The average and standard deviation values are calculated from the differences between Rq of the coating and the core profile of each tablet.

The roughness difference between coating and core profile can also be characterized by the skewness and kurtosis of both profiles (Figure 8). Similar to the changes in Rq, we also observe a change in Rsk and in Rku, at the middle of the process. A smoother surface of the coated tablet is also supported by the kurtosis values. We would like to remind the reader at this point that kurtosis is a measure for sharpness and a spiky surface will have a high kurtosis value. The kurtosis difference, as shown in Figure 8b, thus highlights that the tablet surface is smoother (less spiky surface) after coating ($Rku_{\text{coating}} < Rku_{\text{core}}$). However, it may be preferable to have a rough tablet core surface, which would provide greater interfacial contact between coating solution and tablet. A rougher surface, and thus a larger surface area, causes stronger adhesion bonds between the tablet and the film (Nadkarni et al., 1975).

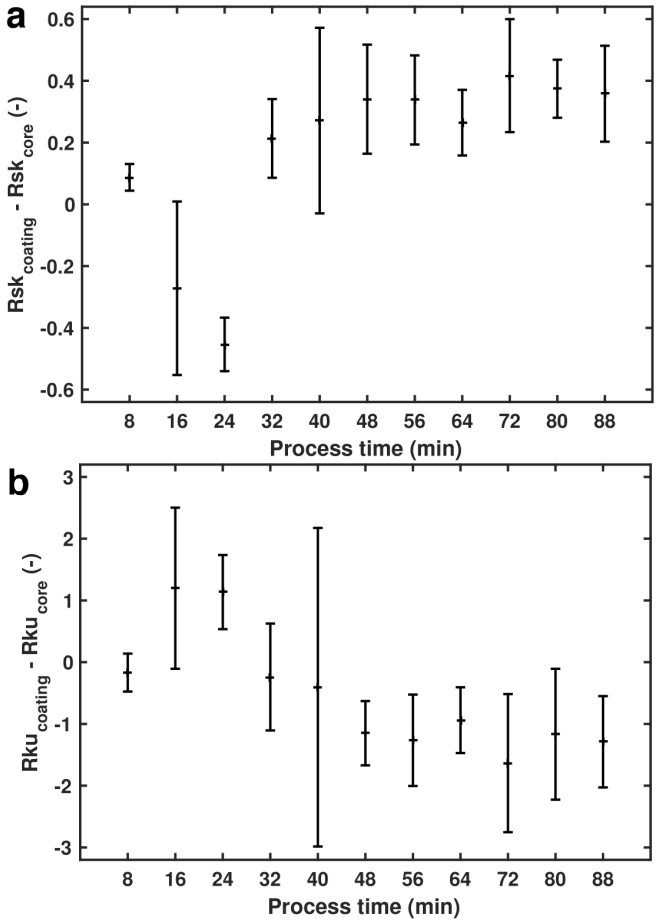

Figure 8: Difference in (a) skewness and (b) kurtosis between coating and core profile.

Figure 9 depicts the skewness of individual tablets drawn from the process at 24 min and 88 min (process end). The skewness of the tablet core is larger at the beginning of the process than that of the coating, whereas the absolute value of the tablet core skewness is closer to 0 (see data of process time 24 min in Figure 9). In contrast to the beginning of the process, the data follows a normal distribution at the end of the process and is thus more symmetrical (i.e. skewness value is closer to 0). Therefore, at the early stages of the process the coating negatively impacts the surface symmetry by forming additional valleys ($Rsk_{\mathrm{coating}} < Rsk_{\mathrm{core}} < 0$). The coating positively impacts the roughness symmetry at the end of the coating process, as indicated by the skewness of the coating, which is closer to 0 than that of the core profile.

The large standard deviation at process time 40 min is due to a defect in the tablet core, as illustrated in Figure 10. Since the tablets are not the same for different process stages, this defect can only be observed in the results from one tablet drawn from the process at 40 min. The tablet with this defect is also an outlier in the Rsk and in the Rq analysis. However, the kurtosis is highly sensitive to such local and small defects, which could have a major impact on the performance of this tablet. It can be clearly observed, by comparing the tablet core and coating profiles, that the defect is in the tablet core. The core profile has a higher value than the coating profile, meaning that negative spikes are filled with coating. However, Rq of the coating and of the core (Figure 7) showed that the final coated surface is in general rougher than the surface of the tablet core, but it is more symmetric and less spiky than the original surface, as indicated by Rsk and Rku.

Such data can be used to gain more insight into the impact of the core roughness on the overall coating uniformity. In particular, analyzing how closely the coated tablet surface follows the uncoated tablet surface strongly depends on the process conditions. It is thus of great interest to have a fast and non-

destructive tool, such as OCT, to investigate the roughness of the tablet core and coating, on the basis of statistical roughness parameters.

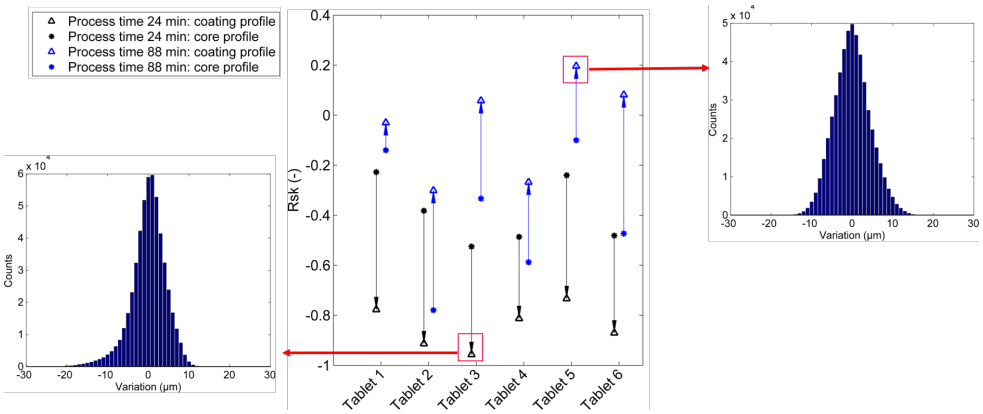

Figure 9: Skewness of six tablets which were randomly drawn from the process after 24 min (black) and after 88 min (blue). The arrows point from the core to the coating value of the same tablet.

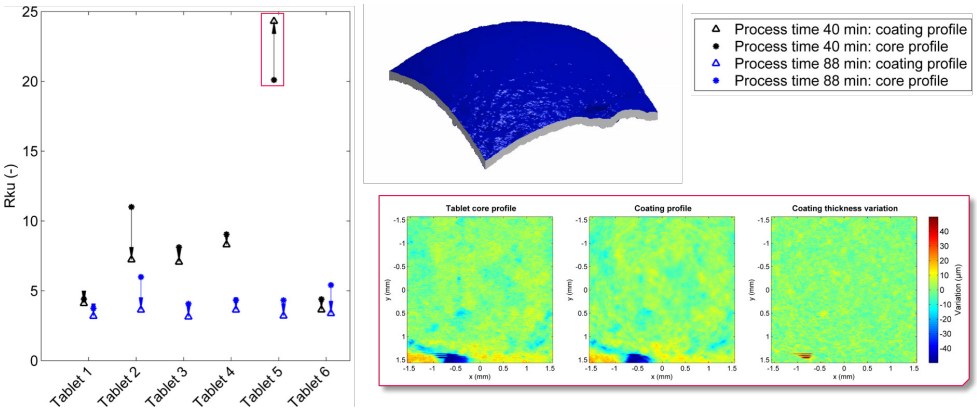

Figure 10: Analysis of a defect in the tablet core and the coating surface. Left figure: Kurtosis of 6 tablets randomly drawn from the coating process after 40 min and at the process completion (88 min). The 3D rendering, as well as the tablet core profile, coating profile and coating thickness variation are data from the tablet highlighted in the red square in the left figure. The arrows point from the core to the coating value of the same tablet.

4. Conclusion

This study reports how the surface roughness evolves during a tablet coating process, by comparing tablet core profile and coating profile using 3D OCT measurements of a part of a tablet face. The data reveal that small valleys are filled with coating, whereas coarse features of the tablet core are visible on the final film-coated tablet. This clearly affects the coating uniformity, as observed in the correlation between the coating thickness variation and the core profile. In addition, the presented concept could be used to detect defects and irregularities in the tablet core, as well as in the coating surface, with one single measurement. Such a detailed investigation cannot be performed with a contact profilometer, which only provides data on the final dosage form surface. In this study we focused on investigating the tablet faces and the results may vary for the tablet band or the surface close to the

edges as it is well known that the coating thickness differs between the tablets faces, the edges and the tablet band. OCT is capable of measuring the tablet band, but it may provide inaccurate measurements of the coating close to the edges.

Moreover, the presented concept could be further transferred to in-line OCT measurements (Markl et al., 2015a), allowing the investigation of core and coating roughness during production. Specifically, for functional and active coatings, slight changes of the coating equipment and process parameters may impact the physicochemical properties of the film, and may thus affect the coating quality. The applicability of OCT to measure functional or active coatings primarily depends on the used coating formulation, which may cause strong scattering losses leading to a reduced penetration depth and limiting the maximum detectable coating thickness.

However, monitoring and controlling coating quality is of great importance to prevent output risks, including batch reprocessing, batch reject and product recall. Characterizing coating properties such as coating thickness, coating uniformity as well as roughness is therefore critical for the purpose of quality control and quality assurance.

ACKNOWLEGMENT

This work has been funded within the Austrian COMET Program under the auspices of the Austrian Federal Ministry of Transport, Innovation and Technology (bmvit), the Austrian Federal Ministry of Economy, Family and Youth (bmwfj) and by the State of Styria (Styrian Funding Agency SFG). COMET is managed by the Austrian Research Promotion Agency FFG.

REFERENCES

Bawuah, P., Mendia, A.P., Silfsten, P., Pääkkönen, P., Ervasti, T., Ketolainen, J., Zeitler, J.A., Peiponen, K.-E., 2014. Detection of porosity of pharmaceutical compacts by terahertz radiation transmission and light reflection measurement techniques. International Journal of Pharmaceutics 465, 70–76. doi:10.1016/j.ijpharm.2014.02.011

Felton, L.A., 2013. Mechanisms of polymeric film formation. Int J Pharm 457, 423–427. doi:10.1016/j.ijpharm.2012.12.027

Juuti, M., Tuononen, H., Prykäri, T., Kontturi, V., Kuosmanen, M., Alarousu, E., Ketolainen, J., Myllylä, R., Peiponen, K.-E., 2009. Optical and terahertz measurement techniques for flat-faced pharmaceutical tablets: a case study of gloss, surface roughness and bulk properties of starch acetate tablets. Measurement Science and Technology 20, 015301. doi:10.1088/0957-0233/20/1/015301

Klukkert, M., Wu, J.X., Rantanen, J., Rehder, S., Carstensen, J.M., Rades, T., Leopold, C.S., 2015. Rapid Assessment of Tablet Film Coating Quality by Multispectral UV Imaging. AAPS PharmSciTech 17, 958–967. doi:10.1208/s12249-015-0414-x

Li, C., Zeitler, J.A., Dong, Y., Shen, Y.-C., 2014. Non-Destructive Evaluation of Polymer Coating Structures on Pharmaceutical Pellets Using Full-Field Optical Coherence Tomography. Journal of Pharmaceutical Sciences 103, 161–166. doi:10.1002/jps.23764

Lin, H., Dong, Y., Shen, Y., Zeitler, J.A., 2015. Quantifying Pharmaceutical Film Coating with Optical Coherence Tomography and Terahertz Pulsed Imaging: An Evaluation. Journal of Pharmaceutical Sciences 104, 3377–3385. doi:10.1002/jps.24535

Lin, H., Dong, Y., Markl, D., Williams, B.M., Zheng, Y., Shen, Y., Zeitler, J.A., 2017. Measurement of the Intertablet Coating Uniformity of a Pharmaceutical Pan Coating Process With Combined Terahertz and Optical Coherence Tomography In-Line Sensing. Journal of Pharmaceutical Sciences 106(4), 1075-1084. doi:10.1016/j.xphs.2016.12.012

Markl, D., Hannesschläger, G., Sacher, S., Leitner, M., Buchsbaum, A., Pescod, R., Baele, T., Khinast, J.G., 2015a. In-Line Monitoring of a Pharmaceutical Pan Coating Process by Optical Coherence Tomography. Journal of Pharmaceutical Sciences 104, 2531–2540. doi:10.1002/jps.24531

Markl, D., Hannesschläger, G., Sacher, S., Leitner, M., Khinast, J., Buchsbaum, A., 2015b. Automated pharmaceutical tablet coating layer evaluation of optical coherence tomography images. Measurement Science and Technology 26, 1–12. doi:10.1088/0957-0233/26/3/035701

Markl, D., Zettl, M., Hannesschläger, G., Sacher, S., Leitner, M., Buchsbaum, A., Khinast, J.G., 2015c. Calibration-free in-line monitoring of pellet coating processes via optical coherence tomography. Chemical Engineering Science 125, 200–208. doi:10.1016/j.ces.2014.05.049

Nadkarni, P.D., Kildsig, D.O., Kramer, P.A., Banker, G.S., 1975. Effect of surface roughness and coating solvent on film adhesion to tablets. Journal of Pharmaceutical Sciences 64, 1554–1557. doi:10.1002/jps.2600640931

Ortiz, S., Siedlecki, D., Grulkowski, I., Remon, L., Pascual, D., Wojtkowski, M., Marcos, S., 2010. Optical distortion correction in Optical Coherence Tomography for quantitative ocular anterior segment by three-dimensional imaging. Optics Express 18, 2782–2796. doi:10.1364/OE.18.002782

Riippi, M., Antikainen, O., Niskanen, T., Yliruusi, J., 1998. The effect of compression force on surface structure, crushing strength, friability and disintegration time of erythromycin acistrate tablets. European Journal of Pharmaceutics and Biopharmaceutics 46, 339–345. doi:10.1016/S0939-6411(98)00043-5

Rowe, R.C., 1979. Surface roughness measurements on both uncoated and film-coated tablets. Pharmacy and Pharmacology Communications 31, 473–474. doi:10.1111/j.2042-7158.1979.tb13557.x

Rowe, R.C., 1978. The measurement of the adhesion of film coatings to tablet surfaces: the effect of tablet porosity, surface roughness and film thickness. Journal of Pharmacy and Pharmacology 30, 343–346. doi:10.1111/j.2042-7158.1978.tb13252.x

Ruotsalainen, M., Heinämäki, J., Guo, H., Laitinen, N., Yliruusi, J., 2003. A novel technique for imaging film coating defects in the film-core interface and surface of coated tablets. European Journal of

362 Pharmaceutics and Biopharmaceutics 56, 381–388. doi:10.1016/S0939-6411(03)00118-8
363 Seitavuopio, P., Heinämäki, J., Rantanen, J., Yliruusi, J., 2006. Monitoring tablet surface roughness
364 during the film coating process. AAPS PharmSciTech 7, E1–E6. doi:10.1208/pt070231
365 Seitavuopio, P., Rantanen, J., Yliruusi, J., 2003. Tablet surface characterisation by various imaging
366 techniques. Int J Pharm 254, 281–286. doi:10.1016/S0378-5173(03)00026-7
367 Twitchell, A.M., Hogan, J.E., Aulton, M.E., 1995. Assessment of the thickness variation and surface
368 roughness of aqueous film coated tabelts using a ligh-section microscope. Drug Development
369 and Industrial Pharmacy 21, 1611–1619. doi:10.3109/03639049509069251
370 Wieser, W., Biedermann, B. R., Klein, T., Eigenwillig, C. M., Huber, R, 2010. Multi-Megahertz OCT:
371 High quality 3D imaging at 20 million A-scans and 45 GVoxels per second. Optics Express 18,
372 14685. doi:10.1364/OE.18.014685
373 Zeitler, J.A., Shen, Y., Baker, C., Taday, P.F., Pepper, M., Rades, T., 2007. Analysis of Coating
374 Structures and Interfaces in Solid Oral Dosage Forms by Three Dimensional Terahertz Pulsed
375 Imaging. Journal of Pharmaceutical Sciences 96, 330–340. doi:10.1002/jps.20789
376